

NASA Technical Memorandum 87825

Satellite-Derived Ice Data Sets No. 2:
Arctic Monthly Average Microwave Brightness
Temperatures and Sea Ice Concentrations,
1973-1976

C. L. Parkinson, J. C. Comiso and H. J. Zwally

MAY 1987

NASA

(NASA-TM-87825) SATELLITE-DERIVED ICE DATA
SETS NO. 2: ARCTIC MONTHLY AVERAGE MICROWAVE
BRIGHTNESS TEMPERATURES AND SEA ICE
CONCENTRATIONS, 1973-1976 (NASA) 43 p
Avail: NTIS HC A03/MF A01

N87-30021

Unclas
0103496

CSCS 08L G3/48

NASA Technical Memorandum 87825

Satellite-Derived Ice Data Sets No. 2:
Arctic Monthly Average Microwave Brightness
Temperatures and Sea Ice Concentrations,
1973-1976

C. L. Parkinson, J. C. Comiso and H. J. Zwally
*Goddard Space Flight Center
Greenbelt, Maryland*



National Aeronautics
and Space Administration

Scientific and Technical
Information Branch

1987

SATELLITE-DERIVED ICE DATA SETS NO. 2:
ARCTIC MONTHLY AVERAGE MICROWAVE BRIGHTNESS TEMPERATURES
AND SEA ICE CONCENTRATIONS, 1973-1976

C. L. Parkinson, J. C. Comiso, and H. J. Zwally
Goddard Laboratory for Oceans

ABSTRACT

This report describes the availability on magnetic tape of a summary data set for four years of Arctic sea ice conditions in the mid 1970s. This data set was derived from brightness temperature data collected by the Electrically Scanning Microwave Radiometer (ESMR) on board the Nimbus 5 satellite over the period 1973 through 1976. The data included on the tape are gridded into 293 by 293 grids that cover a polar stereographic map enclosing the 50°N latitude circle. The grid size varies from about 32 kilometers by 32 kilometers at the poles to about 28 kilometers by 28 kilometers at 50°N. The variables included are the following: (a) monthly averaged microwave brightness temperatures for January, February, June, and July of 1973, September 1973 through May 1975, and September 1975 through October 1976; (b) monthly averages of an ice concentration parameter calculated from the brightness temperatures together with mean climatological atmospheric temperatures; (c) multiyear monthly averages of the brightness temperatures and the ice concentration parameter; (d) yearly and four-yearly averages of the brightness temperatures and the ice concentration parameter; (e) monthly climatological surface air temperatures; and (f) monthly climatological sea level pressures. The ice concentration parameter is calculated assuming the field of view contains only open water and sea ice, with all ice having an emissivity of 0.92. Because first-year sea ice does have an emissivity of approximately 0.92 at the 19-GHz frequency of the ESMR data, the ice concentration parameter represents sea ice concentrations for

regions with exclusively first-year ice and open water. In regions which are complicated by the existence of multiyear ice, which has an emissivity of approximately 0.84, the multiyear ice fractions as well as the ice concentration parameter are needed for the determination of actual ice concentrations. As a result, the values of the ice concentration parameter are termed "pseudo" ice concentrations. A nomogram is presented relating the pseudo ice concentrations to the total ice concentrations and the multiyear ice fractions. Considerations of multiyear ice fraction are not necessary for the determination of ice extents, and consequently maps of monthly and multiyear monthly ice extents from the ESMR data are included at the end of this report.

Detailed analysis of the data and the corresponding Arctic sea ice conditions can be found in the volume Arctic Sea Ice, 1973-1976: Satellite Passive-Microwave Observations by C. L. Parkinson, J. C. Comiso, H. J. Zwally, D. J. Cavalieri, P. Gloersen, and W. J. Campbell. The companion publications for the Antarctic are Satellite-Derived Ice Data Sets No. 1: Antarctic Monthly Average Microwave Brightness Temperatures and Sea Ice Concentrations 1973-1976 by H. J. Zwally, J. C. Comiso, and C. L. Parkinson and Antarctic Sea Ice, 1973-1976: Satellite Passive-Microwave Observations by H. J. Zwally, J. C. Comiso, C. L. Parkinson, W. J. Campbell, F. D. Carsey, and P. Gloersen. The magnetic tapes for both the Arctic and Antarctic data can be obtained from the National Space Science Data Center, Greenbelt, Maryland 20771, or from the World Data Center A for Glaciology, Boulder, Colorado 80309.

SATELLITE-DERIVED ICE DATA SETS NO. 2:
ARCTIC MONTHLY AVERAGE MICROWAVE BRIGHTNESS TEMPERATURES
AND SEA ICE CONCENTRATIONS, 1973-1976

C. L. Parkinson, J. C. Comiso, and H. J. Zwally
Goddard Laboratory for Oceans
NASA/Goddard Space Flight Center
Greenbelt, Maryland 20771

INTRODUCTION

Data from the Electrically Scanning Microwave Radiometer (ESMR) on board the Nimbus 5 satellite have been used to derive information on Arctic sea ice conditions over the four years 1973 through 1976. Detailed analyses of the data and revealed Arctic sea ice cover characteristics are presented in the volume Arctic Sea Ice, 1973-1976: Satellite Passive-Microwave Observations (Parkinson et al., 1987), hereafter referred to as the Arctic atlas or the Arctic sea ice atlas. The Arctic atlas includes false-color images of monthly averaged brightness temperatures at 5 K intervals, monthly averaged ice concentrations at 4-percent intervals, monthly differences in ice concentration at 5-percent intervals, and a wide variety of additional maps and time-sequence plots derived from the microwave data, as well as extensive descriptive analysis.

The ESMR instrument measured radiation at a frequency of 19 GHz and a spatial resolution of approximately 30 kilometers for much of the period from the launch of the Nimbus 5 satellite in December 1972 through March 1983. However, there was a significant reduction in data quality after October 1976 because of degeneration of the instrument, and consequently both this report and the corresponding Arctic sea ice atlas (Parkinson et al., 1987) are restricted to the period January 1973 through October 1976.

The value of the ESMR data for sea ice studies derives from the large contrast in microwave emissivities between sea ice and open water. At the

19-GHz frequency of the ESMR, open water has an emissivity of approximately 0.44 whereas various sea-ice types have emissivities ranging from approximately 0.8 to 0.97. The resulting contrast in microwave brightness temperatures allows conversions to approximate sea ice concentrations (percentages of ocean area covered by sea ice) and hence identification of sea ice distributions throughout the region of observation, as well as temporal variations of these distributions throughout the time period of observation.

The ESMR data set provides the earliest all-weather, all-season imagery of global sea ice. Some satellite data of sea ice in the visible and infrared wavelengths were available in the late 1960s and early 1970s, but visible data cannot be obtained during darkness, and cloud cover often obscures both visible and infrared sensing of the surface, making quantitative estimates of the ice cover difficult. Since the polar regions are either dark or cloud-covered for much of the year, the generation of consistent, long-term data records from visible and infrared sensing is not practical. Accordingly, the passive microwave data collected by the Nimbus 5 ESMR, which are not affected significantly by non-precipitating clouds or by the presence or absence of visible light, introduced a major advance in the usefulness of satellite sea ice imaging and for that reason have been compiled and analyzed in Arctic and Antarctic sea ice atlases (Parkinson et al., 1987; Zwally et al., 1983). The limited resolution of approximately 30 kilometers by 30 kilometers makes the data more suitable for global or other large-scale studies than for small-scale studies. A detailed description of both the Nimbus 5 satellite and the ESMR instrument can be found in the Nimbus 5 User's Guide (Sabatini, 1972).

This report summarizes various aspects of the processing and handling of the Nimbus 5 ESMR data and provides the information necessary for reading and

interpreting the summary data set placed on magnetic tapes made available to the research community.

DATA PROCESSING, COMPILATION, AND MAPPING

The telemetry data from the Nimbus 5 satellite were transmitted to two spaceflight tracking and data network stations located near Fairbanks, Alaska, and Rosman, North Carolina, from which the data were relayed to Goddard Space Flight Center (GSFC). At GSFC, the telemetry data were unpacked, decommutated, supplemented with flags and end of files, and stored on magnetic tapes called experimental tapes (ET's). For data processing convenience, the data from the ESMR instrument were combined from several ET's to form stacked experimental tapes (SET's). The 10-bit telemetry data on the ET's were converted to 32-bit format on the SET's for use on the GSFC computers.

The SET's were used with ephemeris tapes to generate Earth-located calibrated brightness temperature (CBT) tapes, which are the primary source of orbital Earth-located and calibrated radiometer data from the ESMR. The CBT tapes contain the time, calibration parameters, measured brightness temperatures, and corresponding geographical coordinates (Wilheit, 1972). Each CBT tape was written in binary format at 6250 bits per inch and has approximately 180 files, each containing one orbit of data. The tapes are blocked so that each block has 50 records with 560 bytes per record. Table 1 lists the format of each record on a CBT tape.

The Nimbus 5 ESMR recorded radiation from 78 scan positions varying from 50 degrees to the left to 50 degrees to the right of the satellite track (Wilheit, 1972). Full coverage of the entire polar area could be obtained from a sequence of six satellite orbits, or one-half day of good data, if

all 78 beam positions were utilized. However, because of the large disparity in the radiometer field of view from the outer beam position to the middle beam position (70 kilometers by 140 kilometers compared with 25 kilometers by 25 kilometers), generally only the middle 52 beam positions were used, for a swath-angle coverage of ± 30.5 degrees and a minimum resolution of 29 kilometers by 42 kilometers. This swath angle corresponds to a spatial coverage of about 1280 kilometers on the Earth's surface. Because ESMR data from poleward of 85° latitude are obtainable only through use of the outer beam positions, these outer positions, which were otherwise discarded, were used to cover the region between 85° and the poles. Furthermore, because the ESMR senses horizontally polarized radiation, a scan-angle dependent correction was applied to the data to make each observation approximately equivalent to a nadir observation, which is nonpolarized.

With the above restrictions on beam positions and with additional rejection of data because of occasional instrumental problems, about 3 days of data were generally required to provide near-complete spatial coverage of the polar regions. Three-day-average maps were therefore generated for all periods that contained valid data from launch until November 1976. These maps employed a polar stereographic projection, with the data being gridded onto square grids placed over these projections.

Polar stereographic maps are constructed by projecting points on the Earth's surface onto a plane tangent to the surface at either the North Pole or the South Pole, with the vertex of the projection being the opposite pole. The concept is illustrated in Figure 1, where a point B on the Earth's surface is projected to the polar plane at C. The maps used are square grids enclosing the 50°N latitude circle and are gridded to 293×293 grid elements, each

grid element representing an area ranging from about 32 kilometers by 32 kilometers near the poles to about 28 kilometers by 28 kilometers near 50° latitude (Figure 2). The geographical coordinates of the center of the radiometer field of view determine the cell into which the data are placed. Overlapping data in a cell from separate orbits in the same 3-day or monthly period are averaged to give a single brightness temperature taken to be located at the center of the cell.

The coordinates of each element on the projected map are determined as follows: The distance r from the pole to the projected point is calculated as

$$r = d \tan \alpha , \quad (1)$$

where d is the diameter of the Earth, and α is the angular projection at the opposite pole expressed in terms of latitude, ϕ , as

$$\alpha = \frac{\gamma}{2} = \frac{90 - \phi}{2} \quad (2)$$

(Figure 1a). Using the axes and orientation of Figure 1b, the x and y components of the data element with north latitude ϕ and east longitude λ are given by:

$$x = d \tan \left(\frac{90^\circ - \phi}{2} \right) \cos (\lambda - 45^\circ) , \quad (3)$$

$$y = d \tan \left(\frac{90^\circ - \phi}{2} \right) \sin (\lambda - 45^\circ) . \quad (4)$$

The standard map used for the images in this volume is overlaid by a 293 by 293 square grid enclosing the 50°N latitude circle. For the coordinate system selected and a scaled value of d equal to 401.78, each point on the map can be expressed by a set of integer coordinates (I,J) defined with integer truncation by:

$$I = 147 - y + 0.5 , \quad (5)$$

$$J = 147 + x + 0.5 . \quad (6)$$

The value of 0.5 in Equations 5 and 6 properly positions the map cell at the center of its geographic location.

DATA INTERPOLATION AND DETERMINATION OF MONTHLY AVERAGES

The 3-day-averaged maps discussed in the previous section were combined to create the monthly averages contained on the magnetic tapes. Because of data loss caused by instrumental, processing, and calibration problems, as many as 20 percent of the data cells in the 293 by 293 grids were empty on some 3-day-averaged maps, this being more frequent after the launch of the Nimbus 6 satellite in June 1975, when Nimbus 5 data became available only every other day. Fortunately, most of these empty cells are located outside the sea ice region. Nonetheless, for proper weighting of data in the monthly averaged maps, various interpolations were made to fill in some of the empty cells in the 3-day-averaged maps. Because the Arctic data have considerably more data gaps than the Antarctic data, a more complete interpolation procedure was necessary for the Arctic atlas than was used for the Antarctic atlas.

To calculate the monthly averaged brightness temperatures for the Arctic, an initial spatial interpolation was carried out on all 3-day-averaged maps.

In this initial interpolation, all missing data points that were within two pixels of good data on two opposite sides (in the x direction, y direction, or diagonally) were filled in with linearly interpolated values. Next, temporal interpolation was performed, with missing data filled in by linear time interpolation whenever there were good data both in either of the two previous 3-day periods and in either of the two subsequent 3-day periods. Following these two sets of interpolations, a calibration adjustment, described in Appendix A of the Arctic sea ice atlas (Parkinson et al., 1987), was made for each 3-day period from May 18 through October 30 of 1976. Then a weighted monthly averaging was performed, followed by a normalization to place the monthly-averaged ocean-temperature peak consistently at 138.3 K. The details of these and other aspects of the data processing can be found in Appendix A of the Arctic atlas.

The monthly average data were combined into 4-year monthly averages by averaging the January data for the four individual years, the February data for the four individual years, and so on. In cases with missing months due to data gaps, the 4-year averages become 3-year or 2-year averages instead. Yearly averages were also calculated, averaging the matrices for the twelve individual months within the year, with missing months filled in by temporal interpolation. Finally, a full 4-year average was made from the four yearly averages, and that as well as the yearly averages, monthly averages, and 4-year monthly averages, is included on the magnetic tapes associated with this technical memorandum.

DETERMINATION OF AN ICE CONCENTRATION PARAMETER

The magnetic tapes contain, in addition to the ESMR brightness temperature data, an ice concentration parameter derived from that data. Variations in the brightness temperature observed over the surface of the Earth are caused by variations in the emissivity of the surface material and variations in physical temperature according to the equation

$$T_B = \epsilon T , \quad (7)$$

valid for the brightness temperature T_B of a uniform surface type with emissivity ϵ and physical temperature T . Within the ice pack, the brightness temperature of a pixel area derives from various sources, including atmospheric contributors as well as the water and ice within the field of view. To a good approximation, in a situation where the ice is of uniform emissivity,

$$T_B = C_W \epsilon_W T_W + C_I \epsilon_I T_I + T_A , \quad (8)$$

where ϵ_W , T_W , and C_W are the emissivity, surface physical temperature, and areal percentage of water, and ϵ_I , T_I , and C_I are the corresponding values for sea ice. T_A is the sum of the atmospheric and other above-surface contributions, including the direct upwelling radiation from the atmosphere, the downwelling radiation reflected by the surface, and the radiation from space reflected by the surface. The atmospheric opacity in the polar regions, estimated to be very small, was neglected.

Recognizing that $C_W + C_I = 1$, the ice concentration, C_I , can be determined from Equation 8 as

$$C_I = \frac{T_B - T_0}{\epsilon_I T_{\text{eff}} - T_0} \quad (9)$$

where $T_0 = \epsilon_W T_W + T_A$ is the measured brightness temperature of the water determined from the data, and $T_{\text{eff}} = T_I + T_A/\epsilon_I$ is the effective surface physical temperature. In the polar regions, the atmospheric contribution to the effective temperature is small because the humidity and the water-vapor content in the atmosphere are very low. Therefore, T_{eff} is taken to be equal to T_I . The appropriate value for T_I is the temperature at the top of the sea ice below the snow cover, because most of the observed radiation emanates from a thin top layer of saline ice.

In the absence of real-time physical temperature data, T_I is estimated from a compilation of climatological surface air temperatures (also included on the magnetic tapes; see the following section) as follows. The temperature at the top surface of the sea ice is calculated as lying between the surface air temperature, T_{air} , estimated by mean monthly climatological values, and the temperature of the water underneath the ice. The formulation used is

$$T_I = T_{\text{air}} + f (T_F - T_{\text{air}}) , \quad (10)$$

where T_F is the freezing point of sea water (271.2 K), and f is an empirical parameter determined from the observed brightness temperature data by adjusting f until the maximum values of C_I from Equation 9 are consistently about 100 percent during winter. A value of $f = 0.25$ was determined for use in the Antarctic atlas (Zwally et al., 1983), through examination of the July 1974 data over the southern ocean. Later examination of the Northern Hemisphere data showed that $f = 0.25$ is also appropriate for the Arctic. This value of 0.25 agrees with the overall average of surface measurements made at Pond Inlet in the Canadian Archipelago (R. Ramseier, personal communication). In reality,

the magnitude of f will vary spatially with the thicknesses of the ice and the snow cover, but $f = 0.25$ appears to be a reasonable average value.

Analysis of brightness temperatures from the open-ocean area in the vicinity of the ice pack allowed determination of T_0 for use in Equation 9. Specifically, the 4-year-average brightness temperature over ice-free areas of the north polar region was calculated from the ESMR observations to be 138.3 K, and this is the value inserted for T_0 . Of the 138.3 K, approximately 120 K derives from the water and the remainder derives from the atmosphere. [In the Antarctic, the similarly calculated T_0 is 135 K. The 3.3 K difference between hemispheres is believed to be caused predominantly by actual differences in the average signature of ice-free ocean in the two hemispheres. It could also be caused in part by variations in the sensitivity of the instrument with temperature. The satellite is exposed to solar heating as it approaches the north polar region but is not exposed to solar heating as it approaches the south polar region.]

The ice concentration parameter placed on the magnetic tapes is generated from Equation 9 using $T_0 = 138.3$ K, $T_{\text{eff}} = T_I$, as calculated from Equation 10, and $\epsilon_I = 0.92$. The value of 0.92 used for the emissivity is estimated by radiative equations as appropriate for first-year sea ice and is confirmed empirically for first-year ice by examination of the ESMR data. However, many regions of the Arctic contain significant amounts of multiyear ice, which has an emissivity of approximately 0.84 instead of 0.92. Hence the gridded data can be interpreted directly as ice concentrations only in those grid squares containing only open water and first-year sea ice. Otherwise the data should be interpreted using a nomogram (Figure 3), in which both ice concentration, C , and multiyear ice fraction, F_{MY} , are represented as

variables. The crucial element in the generation of the nomogram is the proper placement of the concentration values on the right-hand scale, corresponding to a field of view with exclusively multiyear ice and open water. The right-hand scale on the nomogram was constructed by recognizing that the concentrations C_1 calculated with a first-year ice emissivity were determined by

$$C_1 = \frac{T_B - T_0}{0.92 T_I - T_0} \quad (11)$$

with $T_0 = 138.3$ K, whereas for multiyear ice the calculation would have been

$$C_{MY} = \frac{T_B - T_0}{0.84 T_I - T_0} = C_1 \left(\frac{0.92 T_I - T_0}{0.84 T_I - T_0} \right) . \quad (12)$$

Inserting 248 K as an appropriate overall value for T_I , Equation 12 reduces to $C_{MY} = 1.283 C_1$, which is the conversion used in creating the nomogram of Figure 3. In the Arctic atlas, the ice concentration maps and nomograms are colored-coded, with, for instance, the boundary between light pink and deep brown occurring at 78 percent concentration for first-year ice. From Figure 3, this boundary corresponds to 100 percent ($= 1.283 \times 0.78$) concentration for multiyear ice. Similarly, 44 percent concentration for first-year ice corresponds to 56.5 percent concentration for multiyear ice (Figure 3). This level is colored deep green in the ice concentration maps and nomograms of the atlas. During periods of surface melting, first-year and multiyear ice are indistinguishable by passive microwave measurements (Parkinson et al., 1987), and the appropriate scale for both ice types is the scale on the left of Figure 3. Differences between wet and dry first-year ice, which are about

3 percent, are neglected in the nomogram. The values on tape are termed "pseudo ice concentrations."

In interpreting the pseudo ice concentrations gridded on the magnetic tapes, it is important to realize that the nomogram of Figure 3 should be used and furthermore that a given gridded value is associated with a unique ice concentration only if the multiyear ice fraction F_{MY} is known. For instance, in seasonal sea ice regions with only first-year ice, $F_{MY} = 0$ and the appropriate scale is the scale on the left of the nomogram, so that the gridded values are indeed the calculated ice concentrations. By contrast, in locations where the observed ice field is believed to be totally multiyear ice ($F_{MY} = 1$) then the appropriate scale is on the right-hand side of the nomogram, and the ice concentrations are not the gridded values but those values times 1.283. If no information is known about the multiyear ice fraction, then the nomogram provides the appropriate range of ice concentrations for each gridded value, this range going from the gridded value on the left-hand scale to the value horizontally opposite it on the right-hand scale. For instance, a gridded value of 52 percent indicates an ice concentration anywhere from 52 percent (if there is no multiyear ice) to 67 percent (if the ice is all multiyear ice). The nomogram can also be used in an inverse manner to determine the multiyear ice fraction, if there is independent knowledge (or an estimate) of the total ice concentration. This is done in the Arctic atlas in several cases where the total ice concentration is assumed to be very close to 100 percent.

SURFACE AIR TEMPERATURES AND SEA LEVEL PRESSURES

The data tapes include, in addition to the satellite ESMR brightness temperatures and the derived pseudo sea ice concentrations, matrices of mean monthly climatological surface air temperatures and sea level pressures constructed from data collected over the 30-year period 1931-1960. These data, earlier compiled onto 5° by 5° latitude/longitude grids by Crutcher and Meserve (1970), were obtained on magnetic tapes from Roy Jenne at the National Center for Atmospheric Research and were then regridded to the 293 by 293 polar grids of the ESMR brightness temperatures. The regridding to the finer-resolution grid was done by the following procedure: For each data element in the ESMR grid, the latitude and longitude of the midpoint were calculated. Climatological values at this latitude and two Crutcher and Meserve longitudes 5° apart and on either side of the ESMR longitude were determined using polynomial interpolation of the order 5 on all data from each of the two longitudes. An initial value for the ESMR data element was then inferred by linear interpolation from the two polynomially interpolated values at the same latitude. A second value for the ESMR data element was determined similarly but using polynomially interpolated values at two points at the ESMR longitude but 5° of latitude apart. The two values obtained were usually very close to each other, and their average was used as the final climatological value corresponding to the ESMR data element.

DATA STORAGE AND RETRIEVAL

The gridded data matrices discussed above are stored in sequential arrays on the magnetic tapes associated with this report. For each data matrix D , there is also a population matrix P associated with it. An individual

value $D(I,J)$ in the data matrix represents the average value of the data for grid cell (I,J) , I and J being defined in Equations 5 and 6. For the brightness temperature and ice concentration data matrices, the value $P(I,J)$ in the population matrix corresponding to the value $D(I,J)$ equals the number of measurements averaged to obtain $D(I,J)$. A meaningless population matrix filled with values of 50 is inserted for the surface air temperature and sea level pressure matrices, in order to allow the same format and data sequence to be used for each file of the tapes. In the ice concentration data matrices, land grid points are indicated by values of -50 and, as in the Arctic atlas, all concentrations less than 12 percent are presented as 0 percent.

Table 2 shows the format and the sequence in which the data are stored in each of the files. An 18-word, 4-byte-per-word header preceding each data matrix describes the type of data, the size of the grid, the scaling, the time interval over which the data were accumulated, and other information regarding the recording format (Table 3; this header record, created for the summary data tapes being distributed with this report, differs somewhat from the header records used during the production of the Arctic atlas itself, so that Table 3 is not identical to Table A-5 in Appendix A of the atlas). This header is followed by a sequence of 293 data records interleaved with 293 population records, each record being 293 words long and presenting the values of $D(I,J)$ or $P(I,J)$ for constant I and for J varying from 1 to 293. Each word of the data and population records is 5 bytes, making each record 1465 bytes. On the magnetic tapes, in order to maintain data precision along with an integer format, each data word has been multiplied by a scaling factor of 50. Hence, to obtain brightness temperatures, pseudo ice concentrations,

air temperatures, or pressures, the values on tape must be divided by 50. Although only the first 72 bytes of the header record are meaningful, this record also has a length of 1465 bytes. The data on tape are blocked into 5 records per block. A sample Fortran program and the corresponding job control language for reading the tape on an IBM 3081 computer are given in the Appendix.

All the monthly data have been placed on one magnetic tape written at 6250 bits per inch. The 39 files containing matrices of monthly brightness temperatures from 1973 through 1976 are stored in files 1 through 39 in chronological order, followed by 12 files containing matrices of multiyear monthly brightness temperatures, four files containing matrices of yearly brightness temperatures, and one file containing the matrix of the full 4-year-averaged brightness temperatures. These 56 files are followed by the corresponding 56 files containing pseudo-ice-concentration matrices, the 12 files containing climatological surface air temperature matrices, and the 12 files containing climatological pressure matrices. Table 4 lists the sequence of 136 files, the time interval covered by each file, and both the average population and the overall quality of each brightness temperature and ice concentration matrix. The average population values are lower than those listed in Zwally et al. (1981) for the Antarctic because for the Arctic we have averaged over the whole 293 by 293 grid whereas for the Antarctic the averaging was done only between 55°S and 60°S, where the data are more complete. The Antarctic population values have recently been examined for the entire 293 by 293 grid, and the resulting population averages were found to be comparable to those in Table 4.

A detailed analysis of the data set presented on the magnetic tapes and descriptions of the ice conditions revealed by these data are given in the previously mentioned Arctic sea ice atlas (Parkinson et al., 1987). This atlas includes color-coded images of each of the 136 data matrices on the magnetic tapes, as well as other color-coded images, such as of ice concentration differences from one month to another, and a wide variety of time sequence plots derived from the data. Among the time sequences are plots of the area of ice in various pseudo ice concentration categories for the entire 293 by 293 grid area and for each of eight separate regions. The area of open water, mean ice concentration, and actual ice areas are also shown for the eight regions and the total. Extensive text includes discussion for each of the eight regions of the observed characteristics of the growth-decay cycle and various interannual variations. For convenience in confirming the reading of the magnetic tapes, maps of the monthly and multiyear monthly ice edge positions are included here in Figures 4 through 13.

ACKNOWLEDGMENTS

The authors thank Scott Bringen, Carrie Brezinski, Nick Weiss, and John Liney of Science Applications Research for extensive help in the preparation of the data sets. We also appreciate discussions with Drs. W. J. Campbell, D. J. Cavalieri, F. D. Carsey, and P. Gloersen. This work was supported by NASA's Oceanic Processes Branch.

REFERENCES

- Crutcher, H. L., and J. M. Meserve, 1970: Selected Level Heights, Temperatures, and Dew Points for the Northern Hemisphere, NAVAIR 50-1C-52 (revised), Chief of Naval Operations, Naval Weather Service Command, Washington, D. C., 420 pp.
- Parkinson, C. L., J. C. Comiso, H. J. Zwally, D. J. Cavalieri, P. Gloersen, and W. J. Campbell, 1987: Arctic Sea Ice, 1973-1976: Satellite Passive-Microwave Observations, NASA SP-489, National Aeronautics and Space Administration, Washington, D.C., 296 pp.
- Sabatini, R. R., ed., 1972, Nimbus 5 User's Guide, NASA/Goddard Space Flight Center, Greenbelt, Maryland, 162 pp.
- Wilheit, T. T., 1972: The Electrically Scanning Microwave Radiometer (ESMR) experiment, Nimbus 5 User's Guide, NASA/Goddard Space Flight Center, Greenbelt, Maryland, 59-105.
- Zwally, H. J., J. C. Comiso, and C. L. Parkinson, 1981: Satellite-Derived Ice Data Sets No. 1: Antarctic Monthly Average Microwave Brightness Temperatures and Sea Ice Concentrations 1973-1976, NASA Technical Memorandum 83812, NASA/Goddard Space Flight Center, Greenbelt, Maryland, 34 pp.
- Zwally, H. J., J. C. Comiso, C. L. Parkinson, W. J. Campbell, F. D. Carsey, and P. Gloersen, 1983: Antarctic Sea Ice, 1973-1976: Satellite Passive-Microwave Observations, NASA SP-459, National Aeronautics and Space Administration, Washington, D.C., 206 pp.

Table 1
Data Record Format* for ESMR CBT Tapes

Word Number	Quantity	Units	Scale	Description
1	Year	Year		Year associated with data
2	Day	Days		
3	Hour	Hours		
4	Minute	Minutes		
5	Second	Seconds		
6	Program ID			Unique program identification
7	Pitch error	Degrees	x 10	Pitch fine error
8	Roll error	Degrees	x 10	Roll fine error
9	RMP indicated rate high		x 10	
10	Latitude	Degrees	x 10	Latitude of subsatellite point
11	Longitude	Degrees	x 10	Longitude of subsatellite point
12	Height	Kilometers		Height of spacecraft
13	Hot-load mean		x 10	
14	Hot load		x100	
15	Cold-load mean		x 10	
16	Cold load		x100	
17	MUX 1		x 1	Average antenna temperature
18	MUX 2		x 1	Phase-shift temperature
19	MUX 3		x 1	Ferrite-switch temperature
20	MUX 4		x 1	Ambient-load temperature
21	MUX 5		x 1	Hot-load temperature
22	MUX 6		x 1	Automatic gain control
23-41	Engineering data			
42	Beam position 79			
43-46				Spare
47-124	Latitude	Degrees	x 10	Latitudes of the 78 scan positions
125-202	Longitude	Degrees	x 10	Longitudes of the 78 scan positions
203-280	Brightness temperature	Kelvins	x 10	Brightness temperatures of the 78 scan positions

*Source: Wilheit, 1972.

Table 2

Standard Format* for Each File on the ESMR Monthly Average Data Tapes

(Each file contains a header record, one 293 by 293 data matrix,
and one 293 by 293 population matrix.)

Record Number	Length (bytes)	Format	Number of Words	Description
1	1465	(see below) ⁺	293	Heading (only the first 18 words are meaningful)
2	1465	293I5	293	Row 1 data (x 50)
3	1465	293I5	293	Observation population of row 1
4	1465	293I5	293	Row 2 data (x 50)
5	1465	293I5	293	Observation population of row 2
.
.
.
586	1465	293I5	293	Row 293 data (x 50)
587	1465	293I5	293	Observation population of row 293

*Data format 2 in the header record (see Table 3) indicates standard format.
+(9I5, 2A5, 3I5, 2A5, I5, A5, 255I5, 20I5)

Table 3

Header Record for Each File on the ESMR Monthly Average Data Tapes

Word Number	Format	Number of Bytes/Word	Description
1	I5	4	Projection (1 for polar stereographic)
2	I5	4	Number of columns (293)
3	I5	4	Number of rows (293)
4	I5	4	Scale (25 for $2.5 \times 10^6:1$)
5	I5	4	Latitude enclosed (50°N)
6	I5	4	Greenwich orientation (45°)
7	I5	4	Radius of the Earth in pixels (201)
8	I5	4	J-coordinate of the pole (147)
9	I5	4	I-coordinate of the pole (147)
10-11	2A5	4	Data type* (TB, ICE CON, SURF TEMP, or CLIM PRES)
12	I5	4	File number
13	I5	4	First day of data interval
14	I5	4	Last day of data interval
15	A5	4	Month
16	A5	4	Year**
17	I5	4	Data format (2 for the standard format of Table 2)
18	A5	4	Data identification (ATLS for Arctic Atlas data)
19-293	255I5,20I5	4	Meaningless

*The abbreviations used in words 10 and 11 for the data variables are as follows: TB is brightness temperature, ICE CON is pseudo ice concentration, SURF TEMP is mean monthly climatological surface air temperature, and CLIM PRES is mean monthly climatological sea-level pressure.

**In the case of several-year averages, word 16 indicates the years averaged by the appropriate sequence of last digits. For example, if years 1973, 1974, and 1976 were averaged, word 16 is 346.

Table 4

Files on the ESMR Monthly Average Data Tapes

File Number	Date	Time Interval (Julian Dates)	Average Population	Data Quality
<u>A. ESMR Brightness Temperature Maps</u>				
1	January 1973	001-031	62	Good
2	February 1973	032-059	61	Good
3	June 1973	152-181	62	Good
4	July 1973	182-212	52	Good
5	September 1973	249-273	21	Fair
6	October 1973	274-304	38	Good
7	November 1973	305-332	48	Good
8	December 1973	336-365	50	Good
9	January 1974	001-031	44	Good
10	February 1974	032-059	53	Good
11	March 1974	060-081	41	Good
12	April 1974	097-120	44	Good
13	May 1974	121-151	44	Good
14	June 1974	152-181	54	Good
15	July 1974	182-212	46	Good
16	August 1974	213-243	31	Fair
17	September 1974	244-273	67	Good
18	October 1974	274-304	50	Good
19	November 1974	305-334	52	Good
20	December 1974	335-364	63	Good
21	January 1975	001-028	61	Good
22	February 1975	032-059	46	Good
23	March 1975	060-088	55	Good
24	April 1975	098-106	13	Poor
25	May 1975	122-151	64	Good
26	September 1975	244-273	14	Poor
27	October 1975	274-304	26	Fair
28	November 1975	305-334	24	Fair
29	December 1975	335-365	31	Fair
30	January 1976	001-031	33	Fair
31	February 1976	032-060	31	Fair
32	March 1976	061-091	34	Fair
33	April 1976	092-121	39	Fair
34	May 1976	122-152	34	Fair
35	June 1976	153-182	33	Fair
36	July 1976	186-213	32	Fair
37	August 1976	214-244	40	Fair
38	September 1976	245-274	37	Fair
39	October 1976	275-305	29	Fair

Table 4 (continued)

File Number	Date	Time Interval (Julian Dates)	Average Population	Data Quality
40	January 1973-1976	001-031	200	Good
41	February 1973-1976	032-060	191	Good
42	March 1974-1976	060-091	130	Good
43	April 1974-1976	092-121	96	Fair
44	May 1974-1976	122-152	142	Good
45	June 1973,1974,1976	153-182	149	Good
46	July 1973,1974,1976	183-213	130	Good
47	August 1974,1976	214-244	71	Fair
48	September 1973-1976	245-274	139	Good
49	October 1973-1976	275-305	143	Good
50	November 1973-1975	306-335	124	Good
51	December 1973-1975	336-365	144	Good
52	1973	001-365	394	Fair
53	1974	001-365	589	Good
54	1975	001-365	334	Fair
55	1976	001-366	342	Fair
56	1973-1976	001-366	1659	Good
B. Sea Ice Concentration Maps				
57	January 1973	001-031	62	Good
58	February 1973	032-059	61	Good
59	June 1973	152-181	62	Good
60	July 1973	182-212	52	Good
61	September 1973	249-273	21	Fair
62	October 1973	274-304	38	Good
63	November 1973	305-332	48	Good
64	December 1973	336-365	13	Poor
65	January 1974	001-031	44	Good
66	February 1974	032-059	53	Good
67	March 1974	060-081	41	Good
68	April 1974	097-120	44	Good
69	May 1974	121-151	44	Good
70	June 1974	152-181	54	Good
71	July 1974	182-212	46	Good
72	August 1974	213-243	31	Fair
73	September 1974	244-273	67	Good
74	October 1974	274-304	50	Good
75	November 1974	305-334	52	Good
76	December 1974	335-364	63	Good

Table 4 (continued)

File Number	Date	Time Interval (Julian Dates)	Average Population	Data Quality
77	January 1975	001-028	61	Good
78	February 1975	032-059	46	Good
79	March 1975	060-088	55	Good
80	April 1975	098-106	13	Poor
81	May 1975	122-151	64	Good
82	September 1975	244-273	14	Poor
83	October 1975	274-304	26	Fair
84	November 1975	305-334	24	Fair
85	December 1975	335-365	31	Fair
86	January 1976	001-031	33	Fair
87	February 1976	032-060	31	Fair
88	March 1976	061-091	34	Fair
89	April 1976	092-121	39	Fair
90	May 1976	122-152	34	Fair
91	June 1976	153-182	33	Fair
92	July 1976	186-213	32	Fair
93	August 1976	214-244	40	Fair
94	September 1976	245-274	37	Fair
95	October 1976	275-305	29	Fair
96	January 1973-1976	001-031	200	Good
97	February 1973-1976	032-060	191	Good
98	March 1974-1976	060-091	130	Good
99	April 1974-1976	092-121	96	Fair
100	May 1974-1976	122-152	142	Good
101	June 1973,1974,1976	153-182	149	Good
102	July 1973,1974,1976	183-213	130	Good
103	August 1974,1976	214-244	71	Fair
104	September 1973-1976	245-274	139	Good
105	October 1973-1976	275-305	143	Good
106	November 1973-1975	306-335	124	Good
107	December 1973-1975	336-365	107	Good
108	1973	001-365	357	Fair
109	1974	001-365	589	Good
110	1975	001-365	334	Fair
111	1976	001-366	342	Good
112	1973-1976	001-366	1622	Good

Table 4 (continued)

File Number	Date	Time Interval (Julian Dates)	Average Population	Data Quality
C. Monthly Climatological Surface Temperature Maps				
113	January	001-031		
114	February	032-059		
115	March	060-090		
116	April	091-120		
117	May	121-151		
118	June	152-181		
119	July	182-212		
120	August	213-243		
121	September	244-273		
122	October	274-304		
123	November	305-334		
124	December	335-365		
D. Monthly Climatological Sea Level Pressure Maps				
125	January	001-031		
126	February	032-059		
127	March	060-090		
128	April	091-120		
129	May	121-151		
130	June	152-181		
131	July	182-212		
132	August	213-243		
133	September	244-273		
134	October	274-304		
135	November	305-334		
136	December	335-365		

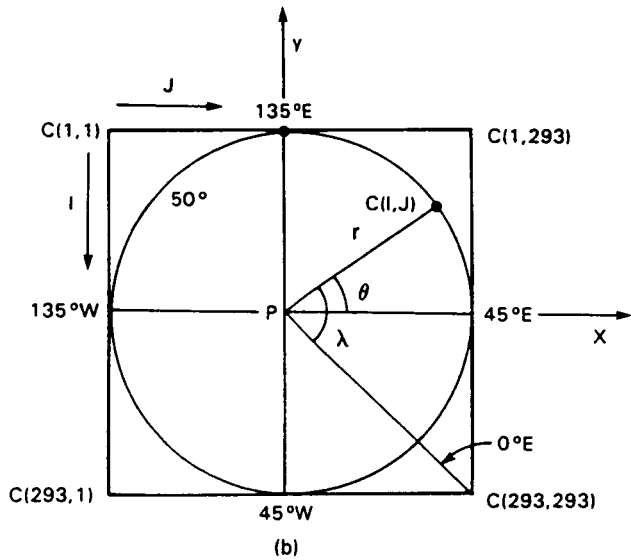
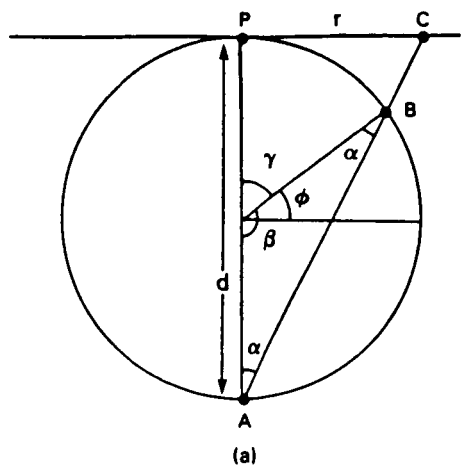


Figure 1. Schematic diagrams for polar stereographic mapping in the Northern Hemisphere.

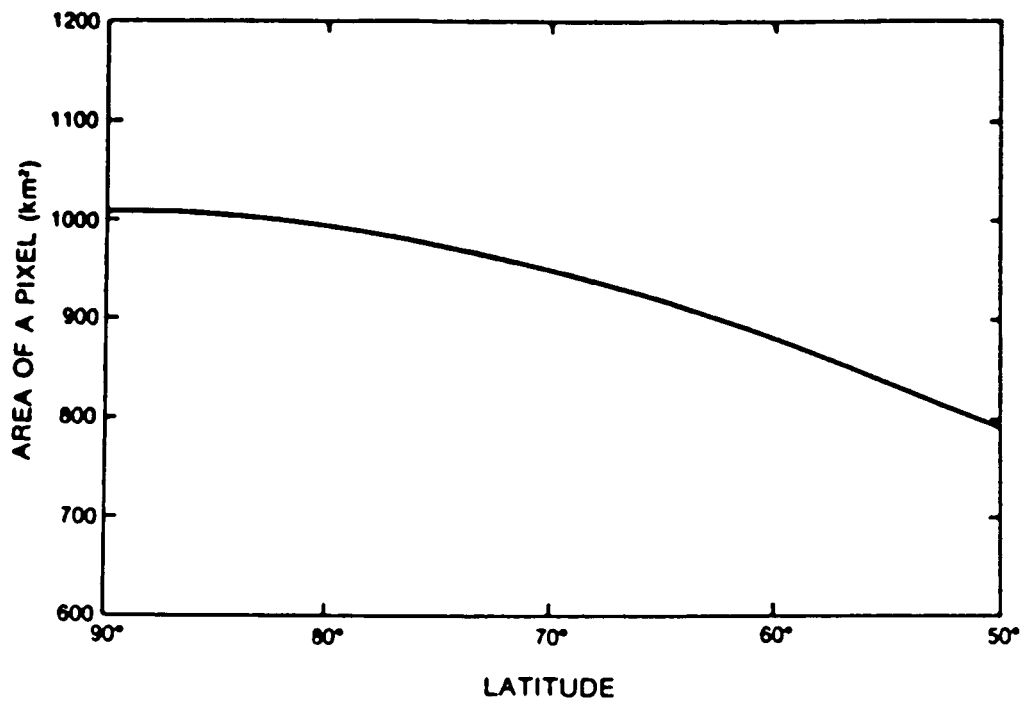


Figure 2. Area of a map element (pixel) as a function of latitude.

ORIGINAL PAGE IS
OF POOR QUALITY

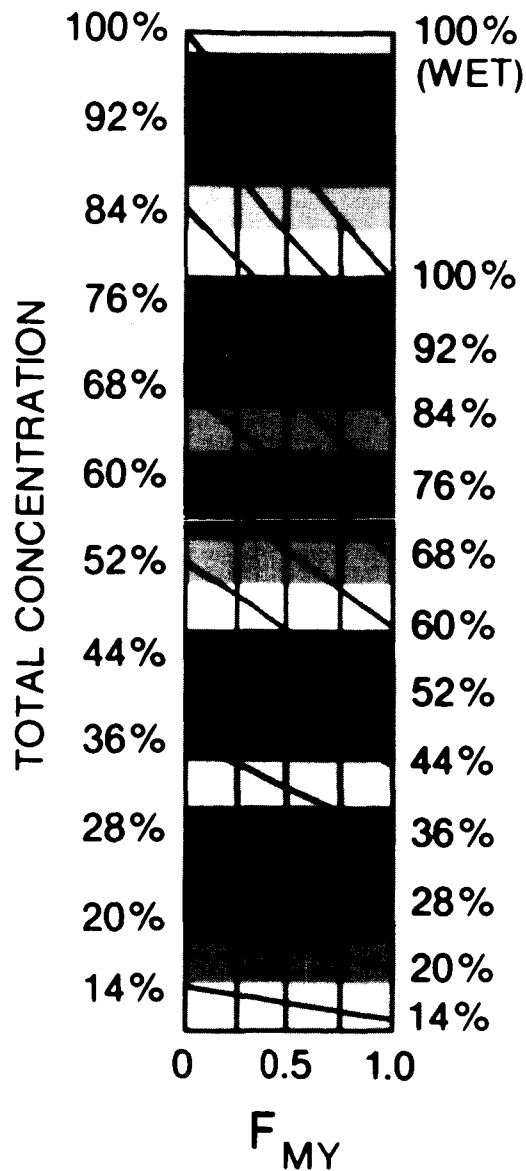


Figure 3. Nomogram of total ice concentration as a function of the ratio F_{MY} of multiyear ice area to total ice area. The ice concentration parameter presented on the magnetic tapes, termed pseudo ice concentration and represented here by the left-hand scale, can be converted to ice concentrations if F_{MY} is known: proceed horizontally from the value on the left-hand scale rightward until the proper value of F_{MY} is reached and then read the total ice concentration from the diagonally slanted lines. For instance, with F_{MY} equal to 0.5 and the pseudo ice concentration equal to 60 %, the total ice concentration is 68 %. In Parkinson et al. (1987), the nomogram is presented in color, with corresponding color-coded maps of the pseudo ice concentrations for the monthly, yearly, and multiyearly averages.

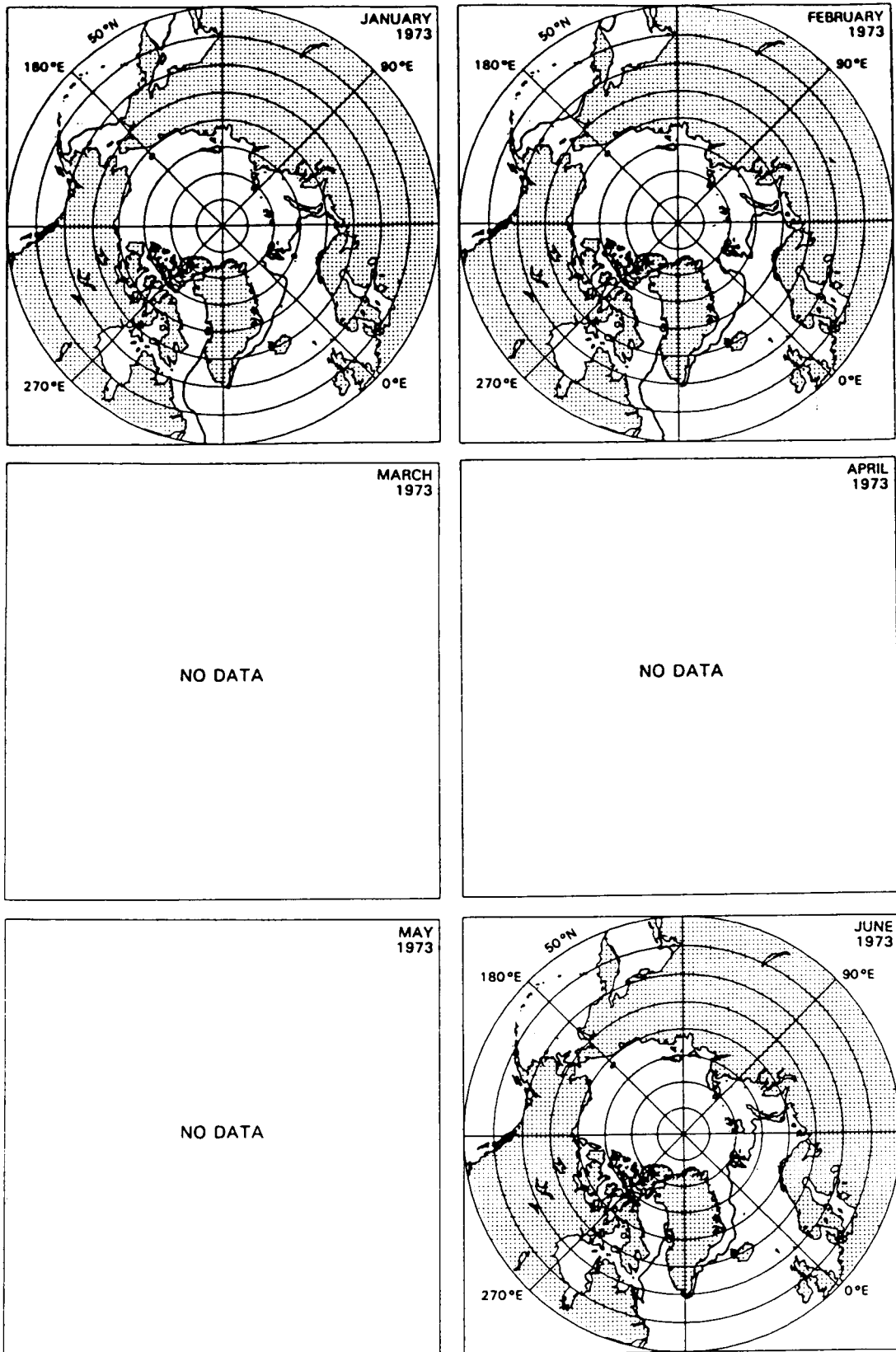


Figure 4. Mean monthly sea ice extents (ice concentrations $\geq 15\%$) for January through June 1973.

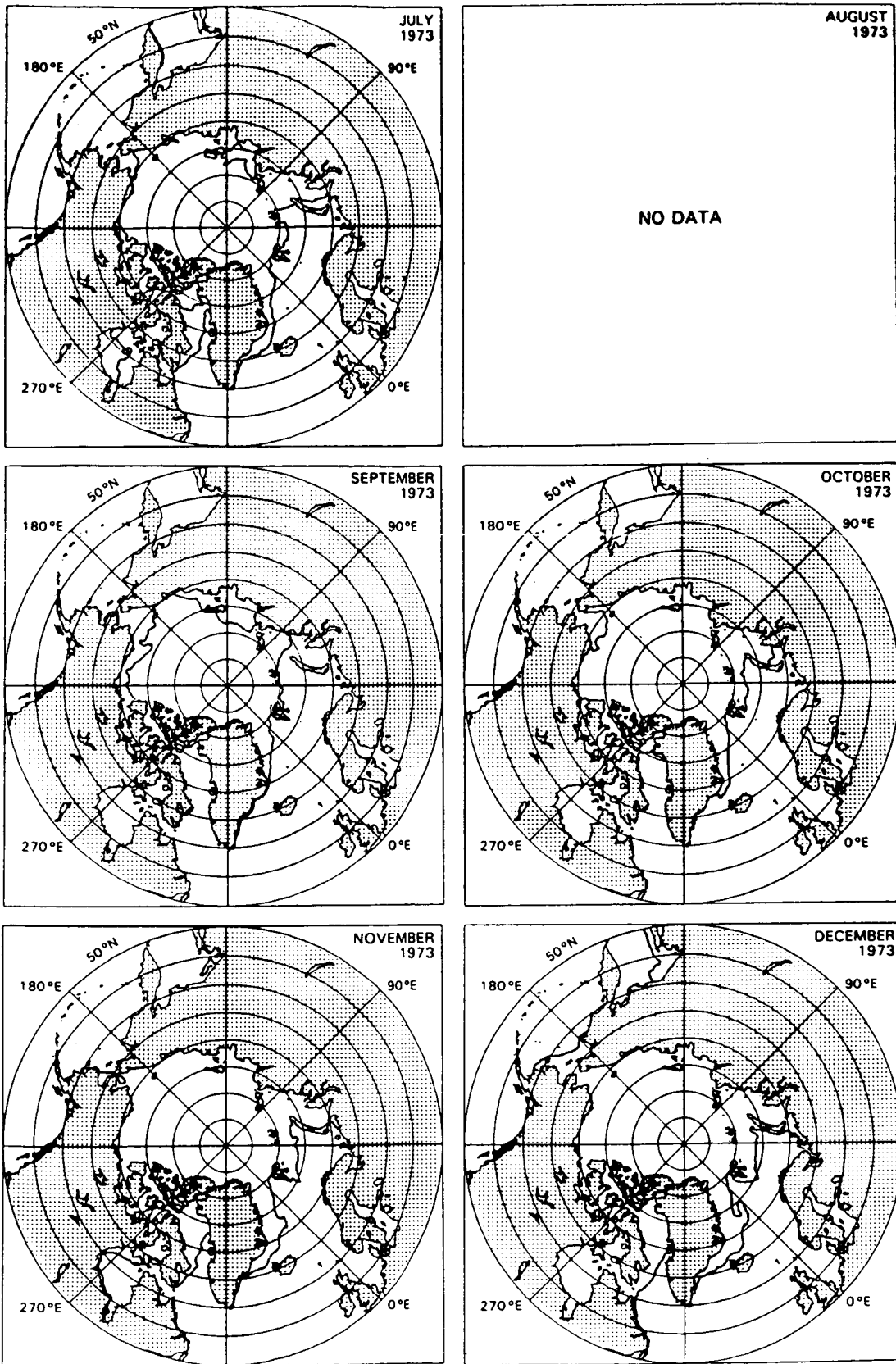


Figure 5. Mean monthly sea ice extents (ice concentrations $\geq 15\%$) for July through December 1973.

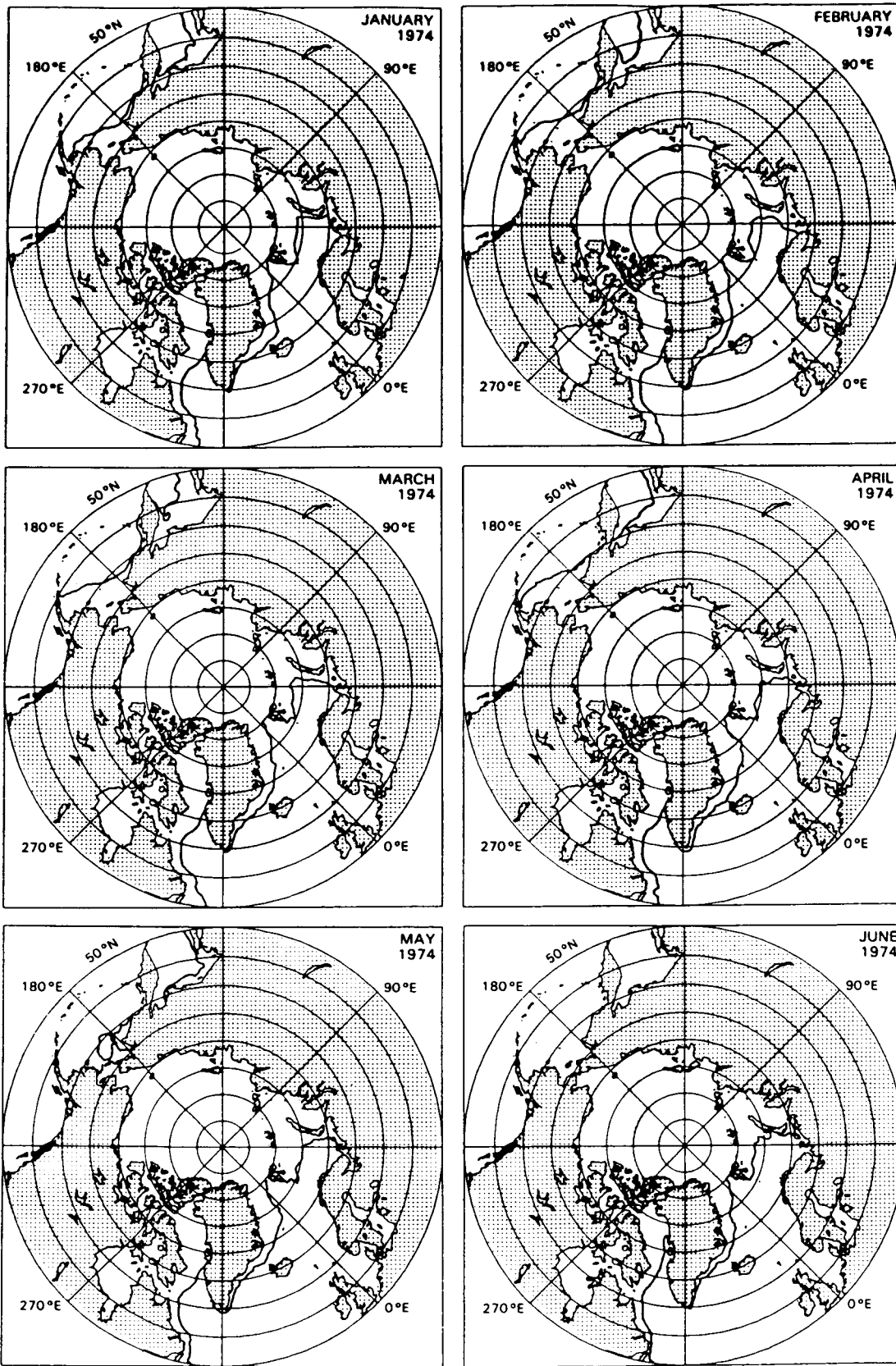


Figure 6. Mean monthly sea ice extents (ice concentrations $\geq 15\%$) for January through June 1974.

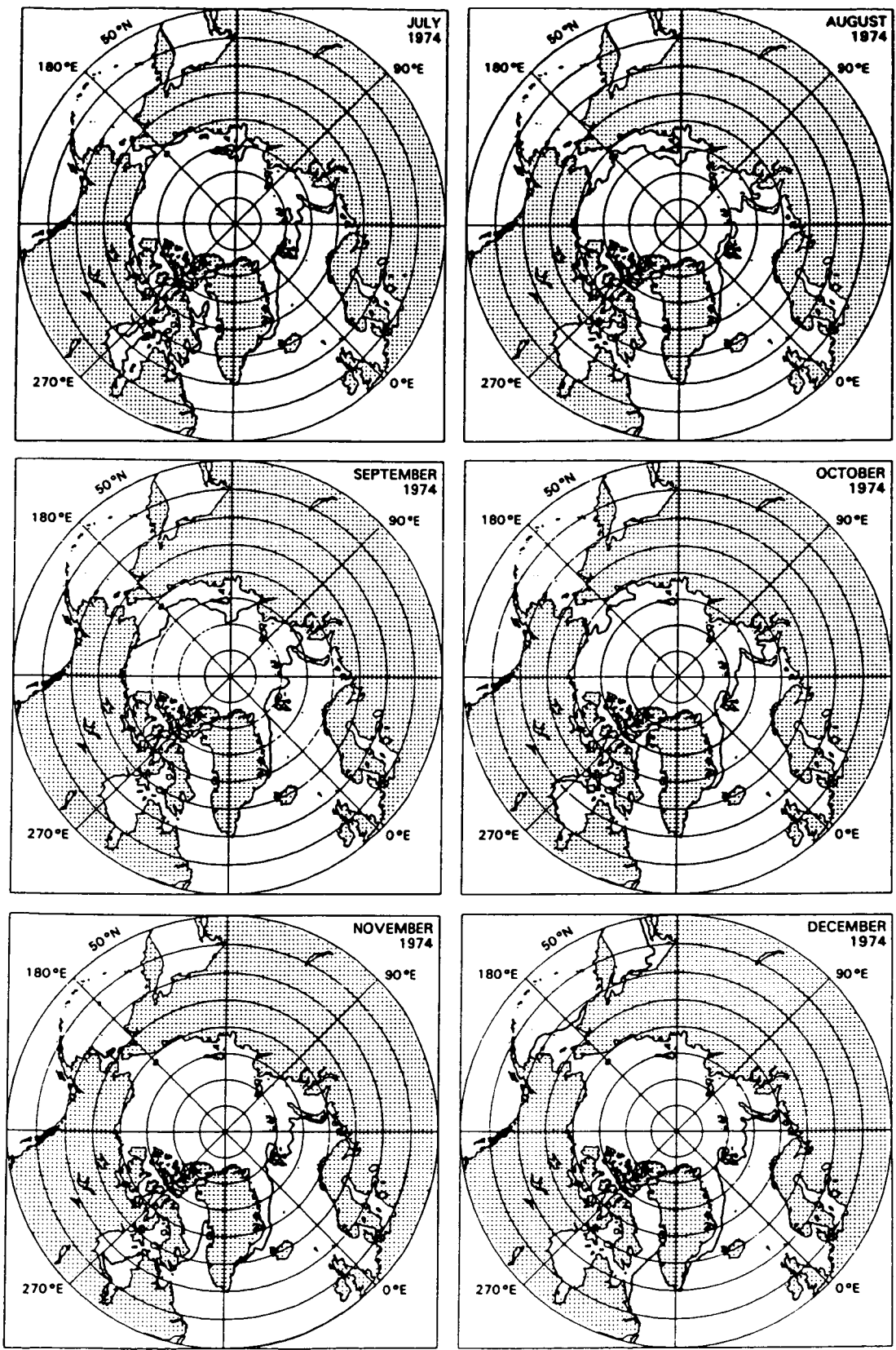


Figure 7. Mean monthly sea ice extents (ice concentrations $\geq 15\%$) for July through December 1974.

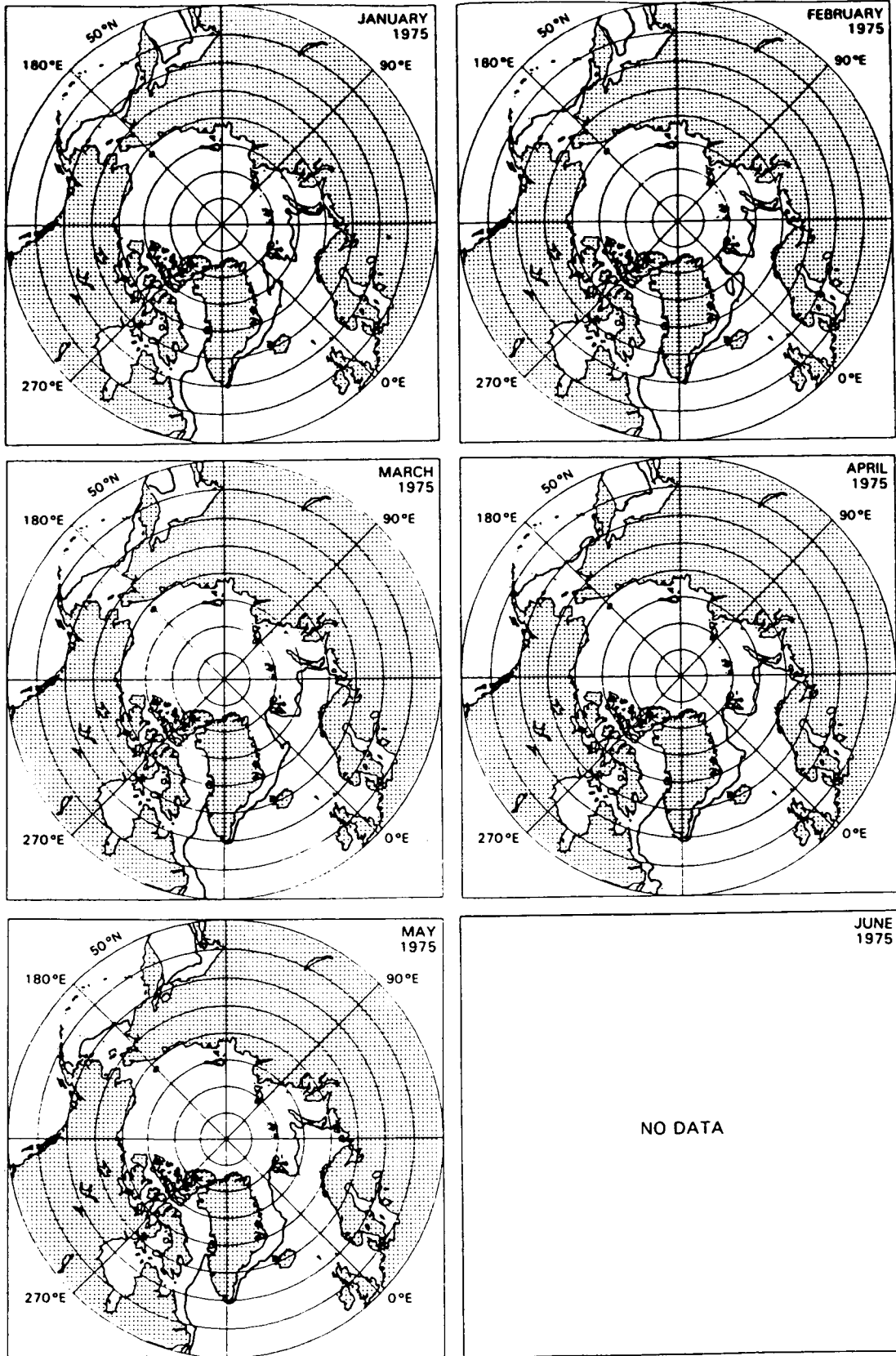


Figure 8. Mean monthly sea ice extents (ice concentrations $\geq 15\%$) for January through June 1975.

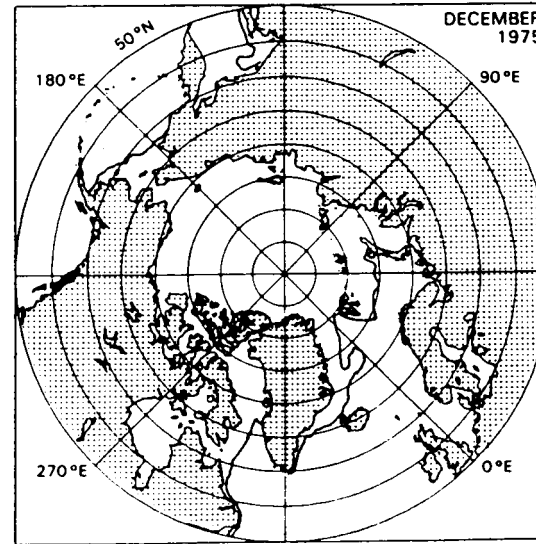
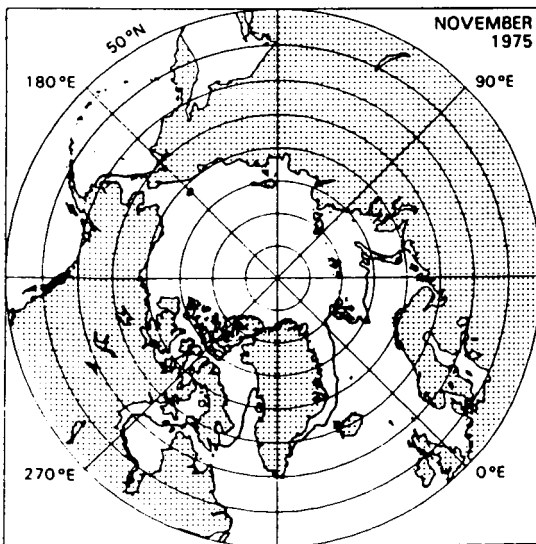
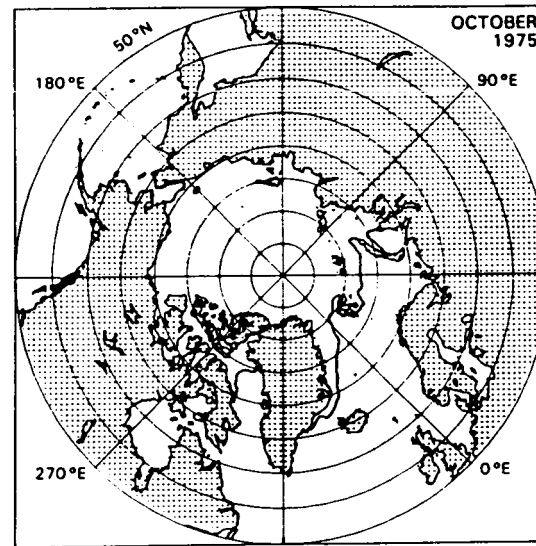
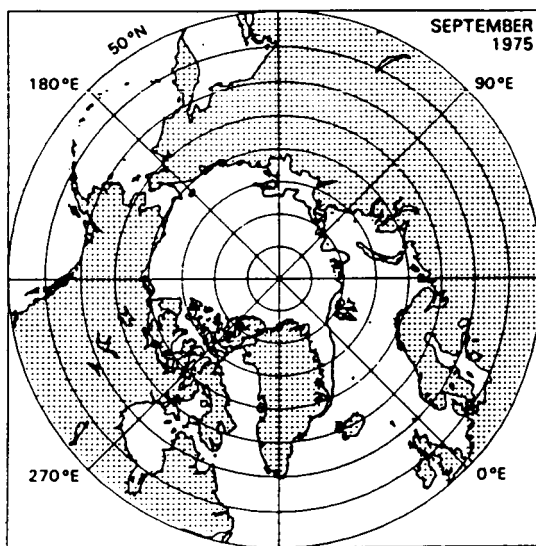
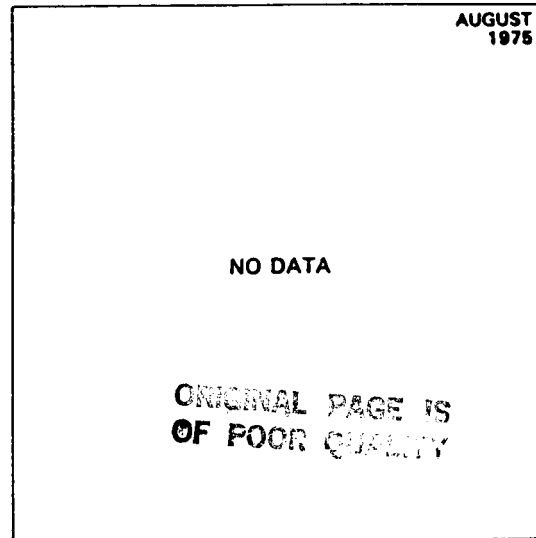
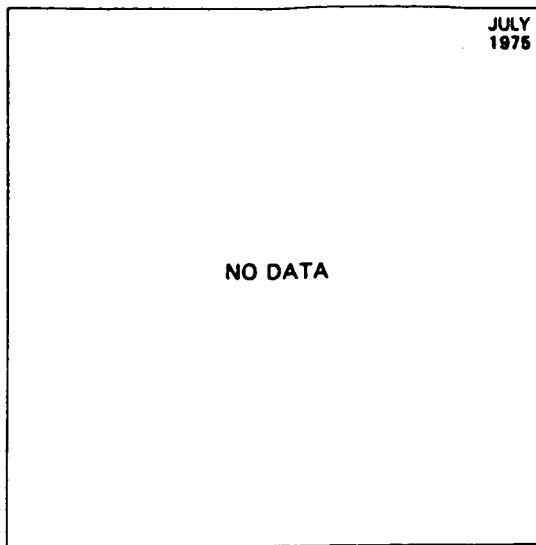


Figure 9. Mean monthly sea ice extents (ice concentrations \geq 15 %) for July through December 1975.

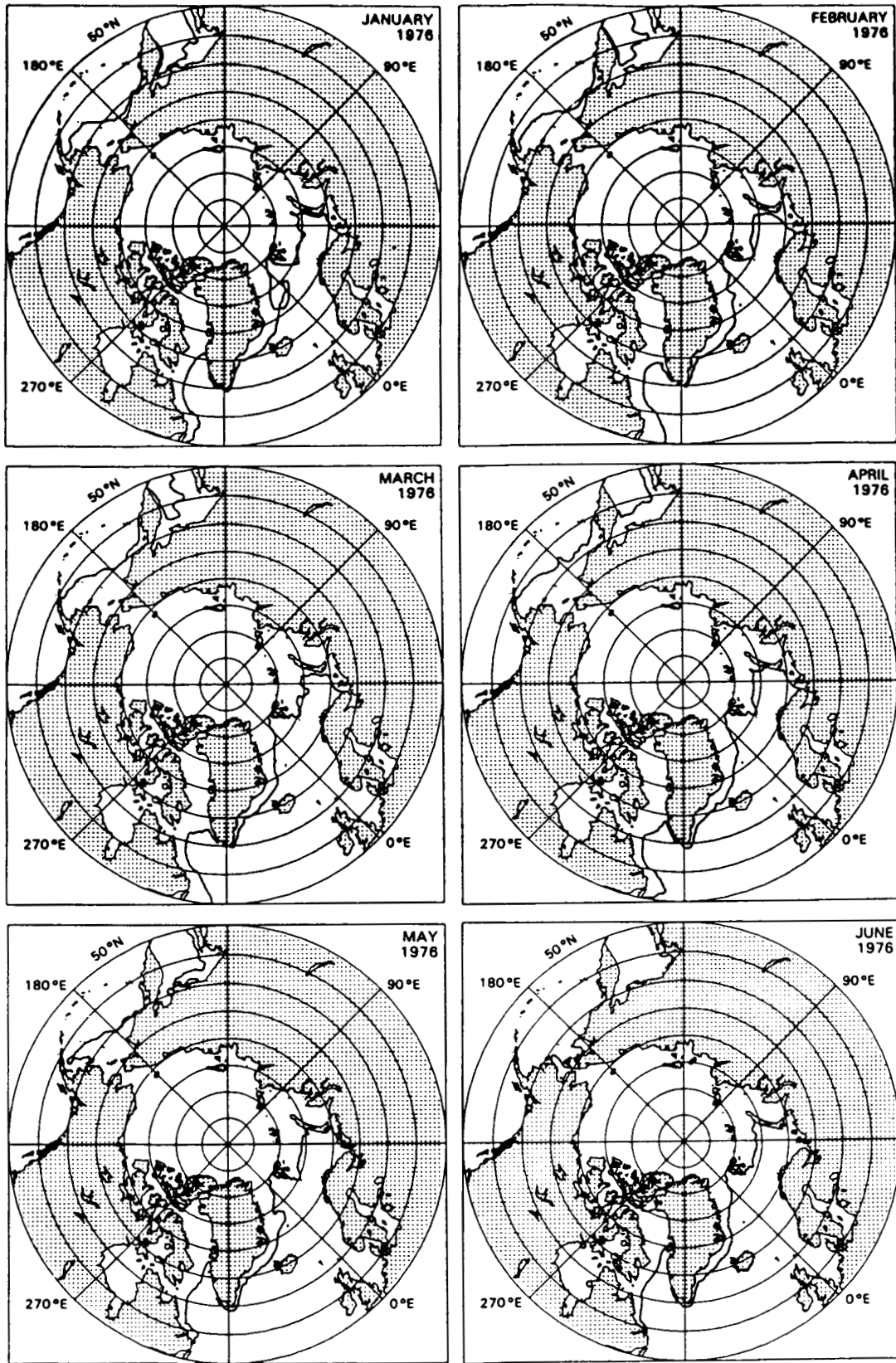


Figure 10. Mean monthly sea ice extents (ice concentrations $\geq 15\%$) for January through June 1976.

ORIGINAL 1976 AS
OF POOR QUALITY

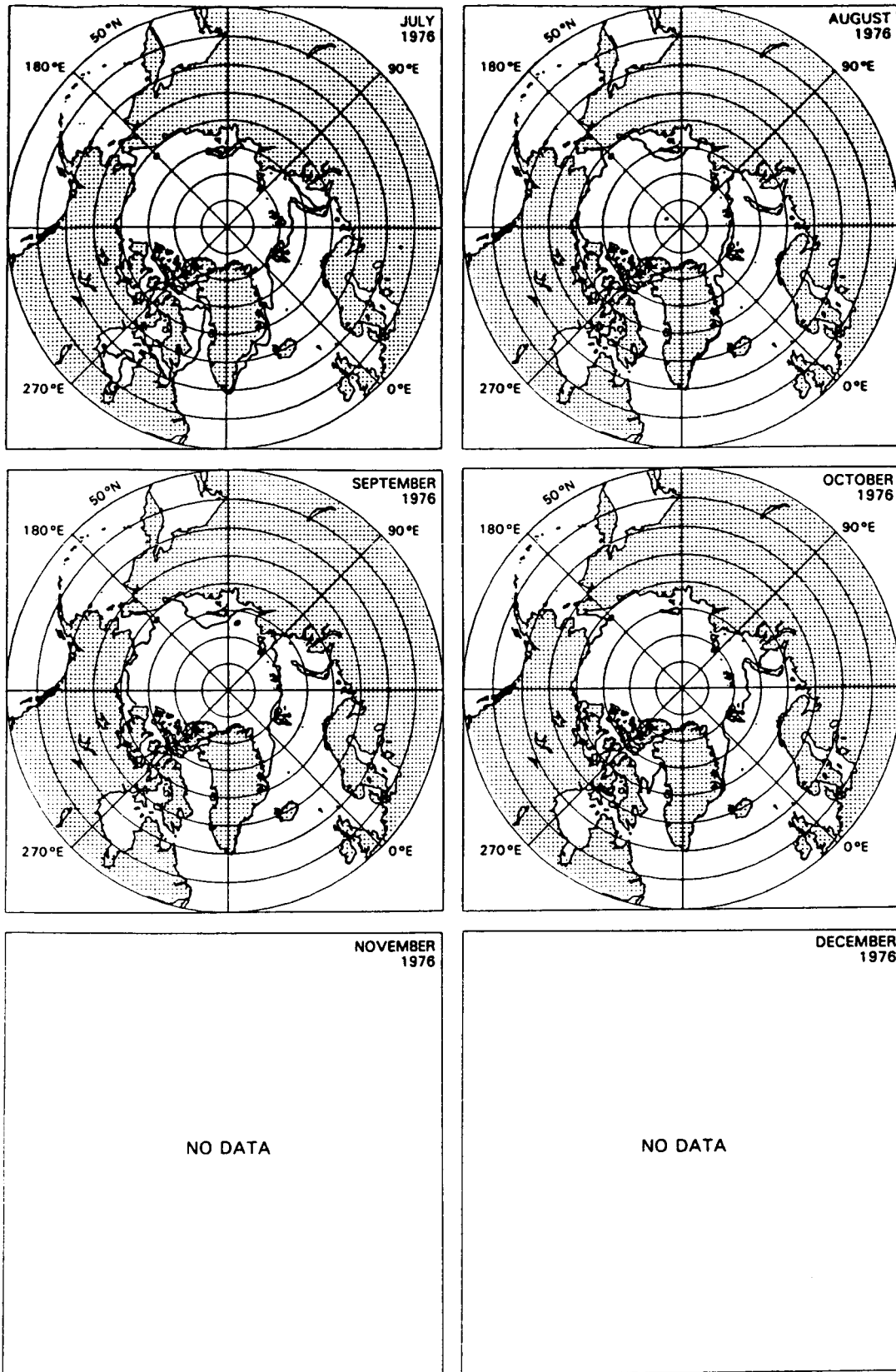


Figure 11. Mean monthly sea ice extents (ice concentrations $\geq 15\%$) for July through December 1976.

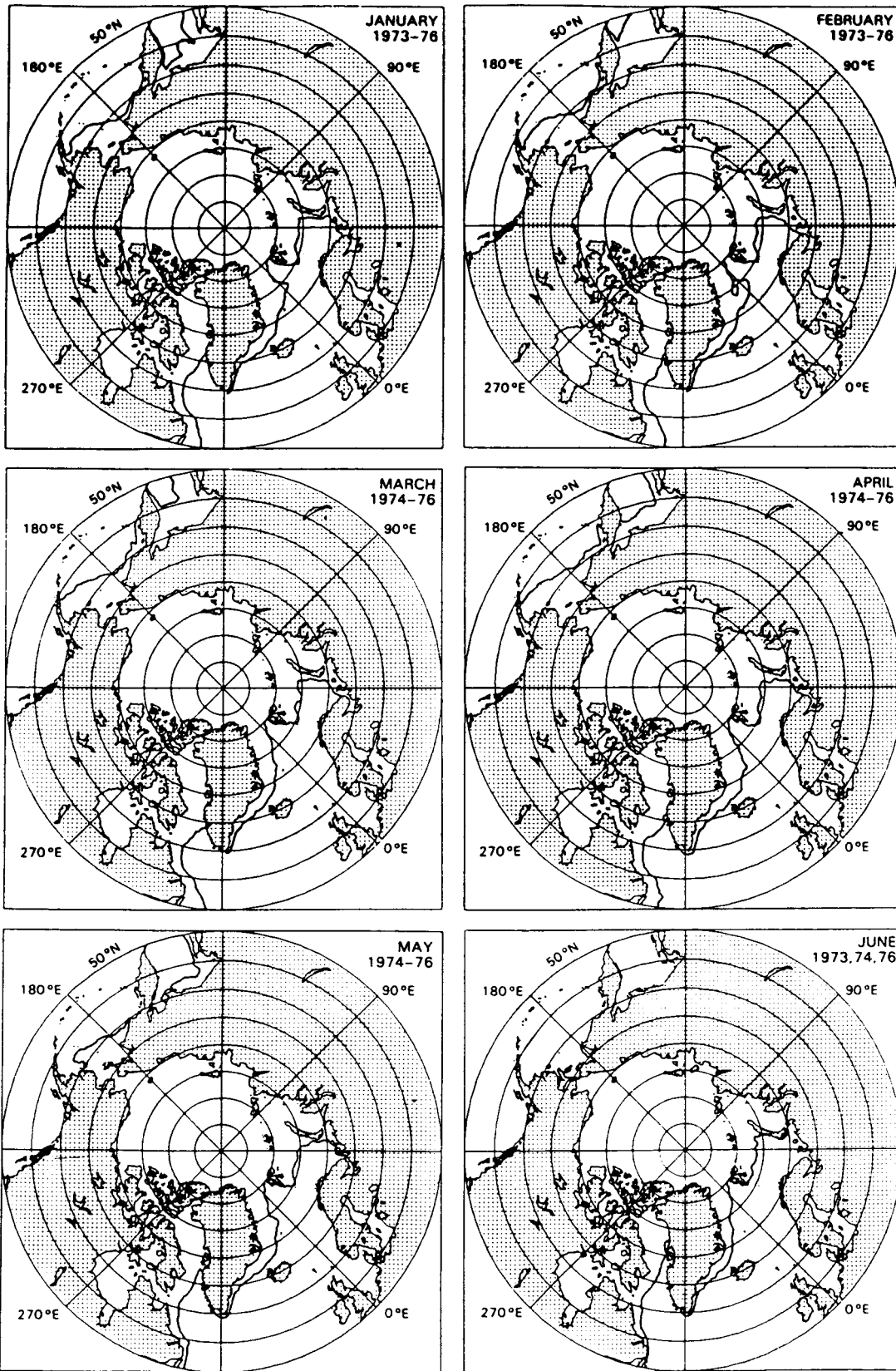


Figure 12. Mean monthly sea ice extents for January through June, averaged for the years indicated.

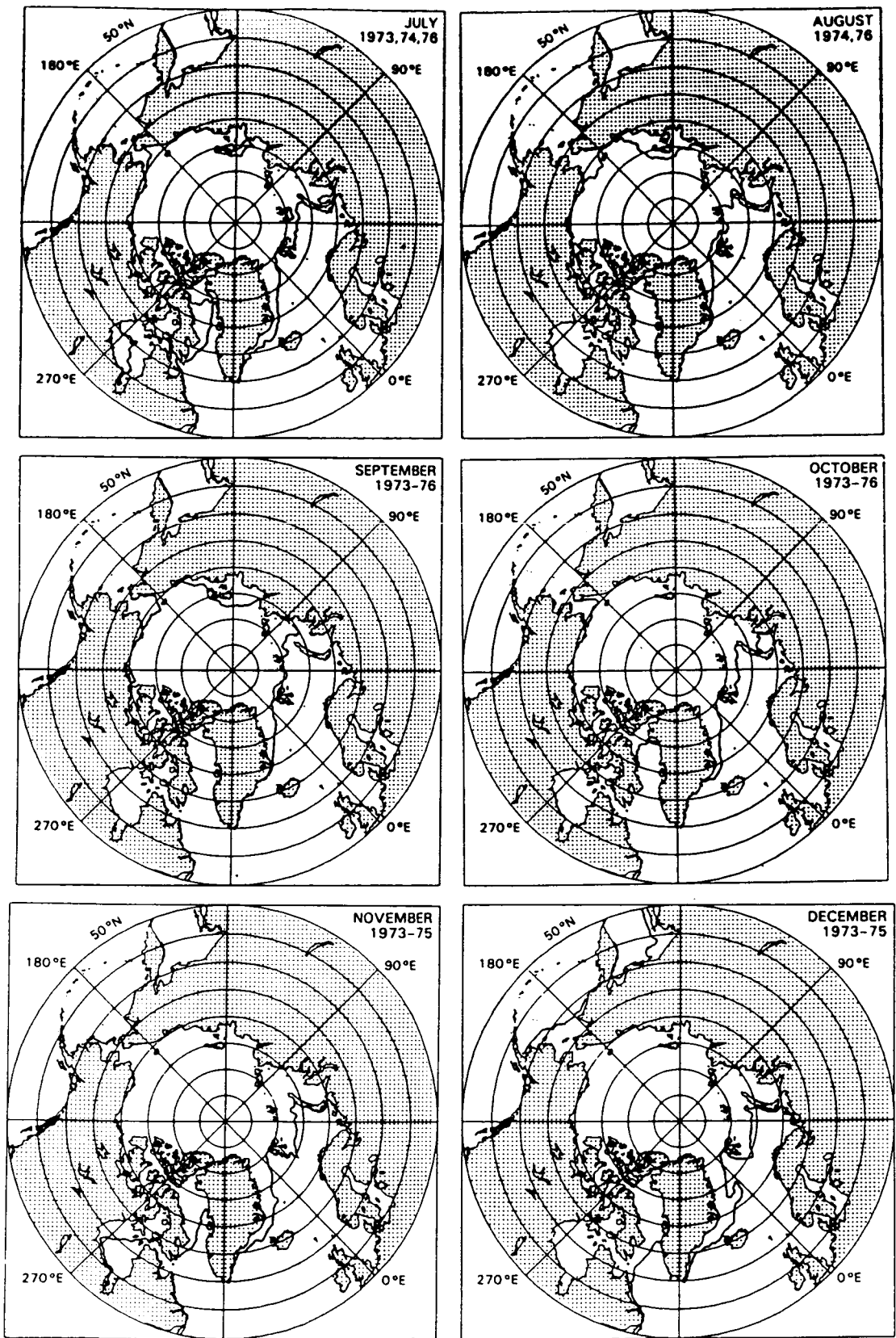


Figure 13. Mean monthly sea ice extents for July through December, averaged for the years indicated.

APPENDIX

I. Sample Fortran program for reading the data tape:

```
DIMENSION IHEAD(293), IDAT(293), IPOP(293)
DO 10 N = 1,136
READ (8,510) IHEAD
DO 50 J = 1,293
READ (8,520) IDAT
READ (8,520) IPOP
50 CONTINUE
10 CONTINUE
510 FORMAT (9I5, 2A5, 3I5, 2A5, I5, A5, 255I5, 20I5)
520 FORMAT (255I5, 38I5)
STOP
END
```

II. Job control language, tape density, and blocking specifications appropriate for reading the data tape on an IBM 3081 computer:

```
//FT08F001 DD UNIT=(6250,,DEFER),LABEL=(1,NL),DISP=OLD,
// DCB=(DEN=4,RECFM=FB,LRECL=1465,BLKSIZE=7325),VOL=SER=xxxx
```

BIBLIOGRAPHIC DATA SHEET

1. Report No. TM-87825	2. Government Accession No.	3. Recipient's Catalog No.	
4. Title and Subtitle Satellite-Derived Ice Data Sets No.2: Arctic Monthly Average Microwave Brightness Temperatures and Sea Ice Concentrations, 1973-1976		5. Report Date May 1987	
		6. Performing Organization Code 67I	
7. Author(s) C. L. Parkinson, J. C. Comiso, H. J. Zwally		8. Performing Organization Report No.	
9. Performing Organization Name and Address Goddard Space Flight Center Greenbelt, MD 20771		10. Work Unit No.	
		11. Contract or Grant No.	
		13. Type of Report and Period Covered Technical Memorandum	
12. Sponsoring Agency Name and Address National Aeronautics and Space Administration Washington, D.C. 20546		14. Sponsoring Agency Code	
15. Supplementary Notes A detailed analysis of the data on the tapes described in this report is included in an atlas entitled "Arctic Sea Ice, 1973-1976: Satellite Passive-Microwave Observations" by C. L. Parkinson, J. C. Comiso, H. J. Zwally, D. J. Cavalieri, P. Gloersen, and W. J. Campbell (NASA SP-489, 1987).			
16. Abstract This report describes the availability on magnetic tape of a summary data set for four years of Arctic sea ice conditions in the mid 1970s. The data include monthly and yearly averaged Nimbus 5 electrically scanning microwave radiometer (ESMR) brightness temperatures, an ice concentration parameter derived from the brightness temperatures, monthly climatological surface air temperatures, and monthly climatological sea level pressures. All data matrices are gridded into 293 by 293 grids that cover a polar stereographic map enclosing the 50°N latitude circle. The grid size varies from about 32 kilometers by 32 kilometers at the poles to about 28 kilometers by 28 kilometers at 50°N. The ice concentration parameter is calculated assuming that the field of view contains only open water and first-year ice with an ice emissivity of 0.92. To account for the presence of multiyear ice, a nomogram is provided relating the ice concentration parameter, the total ice concentration, and the fraction of the ice cover which is multiyear ice. Further analysis and application of the data are encouraged.			
17. Key Words (Selected by Author(s)) Sea Ice Data, Microwave Brightness, Arctic		18. Distribution Statement STAR Category Unclassified-Unlimited	
19. Security Classif. (of this report) Unclassified	20. Security Classif. (of this page) Unclassified	21. No. of Pages 39	22. Price*